*Journal of Electromagnetic Waves and Applications, Vol. 8, No. 4, 489–508, 1994*
© *1994 VSP*

# Finite-difference time-domain formulation of an inverse scattering scheme for remote sensing of inhomogeneous lossy layered media: Part I - One dimensional case

K. Umashankar

Department of Electrical Engineering and Computer Science
University of Illinois at Chicago
Chicago, Illinois 60680, USA

S. Chaudhuri

Department of Electrical Engineering
and Computer Science
University of Waterloo
Waterloo, Ont. N2L 3G1, Canada

A. Taflove

Department of Electrical Engineering and Computer Science
Northwestern University
Evanston, Illinois 60208, USA

**Abstract**–The inverse scattering problem of determining the electromagnetic characteristics, namely, conductivity, permittivity and permeability profiles of an inhomogeneous one-dimensional layered medium is presented in the time domain utilizing the layer-stripping procedure. A fully explicit numerical algorithm is proposed for simultaneous extraction of the electrical parameters by simulating a real-time wave propagation and scattering based on the Finite-Difference Time-Domain method. This yields an efficient profile inversion technique suitable for layered medium synthesis. Examples of the one-dimensional conductivity and permittivity profile inversions are also presented including the depth of the medium probed.

## I. INTRODUCTION

This investigation is concerned with the inverse scattering problem of determining the electromagnetic characteristics, namely, the conductivity, permittivity and permeability $(\sigma, \epsilon, \mu)$ of an isotropic inhomogeneous layered propagation medium from the knowledge of the time-dependent incident wave excitation and the corresponding back-scattered field response. The present discussion deals with only the case of one-dimensional layered medium situations for which both the incident field and the inhomogeneous scatterer medium are one-dimensional. In spite of its simplicity, this situation is often considered as an useful model for many practical applications involving the electromagnetic material synthesis and fabrication of layered structures; probing of biological media and natural geophysical media such

as the earth, ice, sea; case of target identification and/or object reconstruction problems.

The solution of the profile inversion problem, Fig. 1, can be approached on the basis of either the integral equation formulation or the differential equation formulation of the associated direct scattering and propagation problem. Several analytical and numerical methods of profile inversion based on the integral equation formulation – both in the frequency domain and in the time domain – have been discussed in the literature [1–6]. In contrast, to the best of the authors' knowledge, little or no attempt to solve this profile inversion problem with the numerical differential equation formulation has been made. As will be discussed later, the time domain differential equation formulation [7–10] is simple to implement and has broad applications compared to the previously attempted inversion methods. Therefore, in this paper, based on the time-domain solution of the basic Maxwell's coupled curl equations [7, 8], a numerical iterative optimization scheme is presented for the determination of electromagnetic characteristics $(\sigma, \epsilon, \mu)$ of a one-dimensional layered medium.

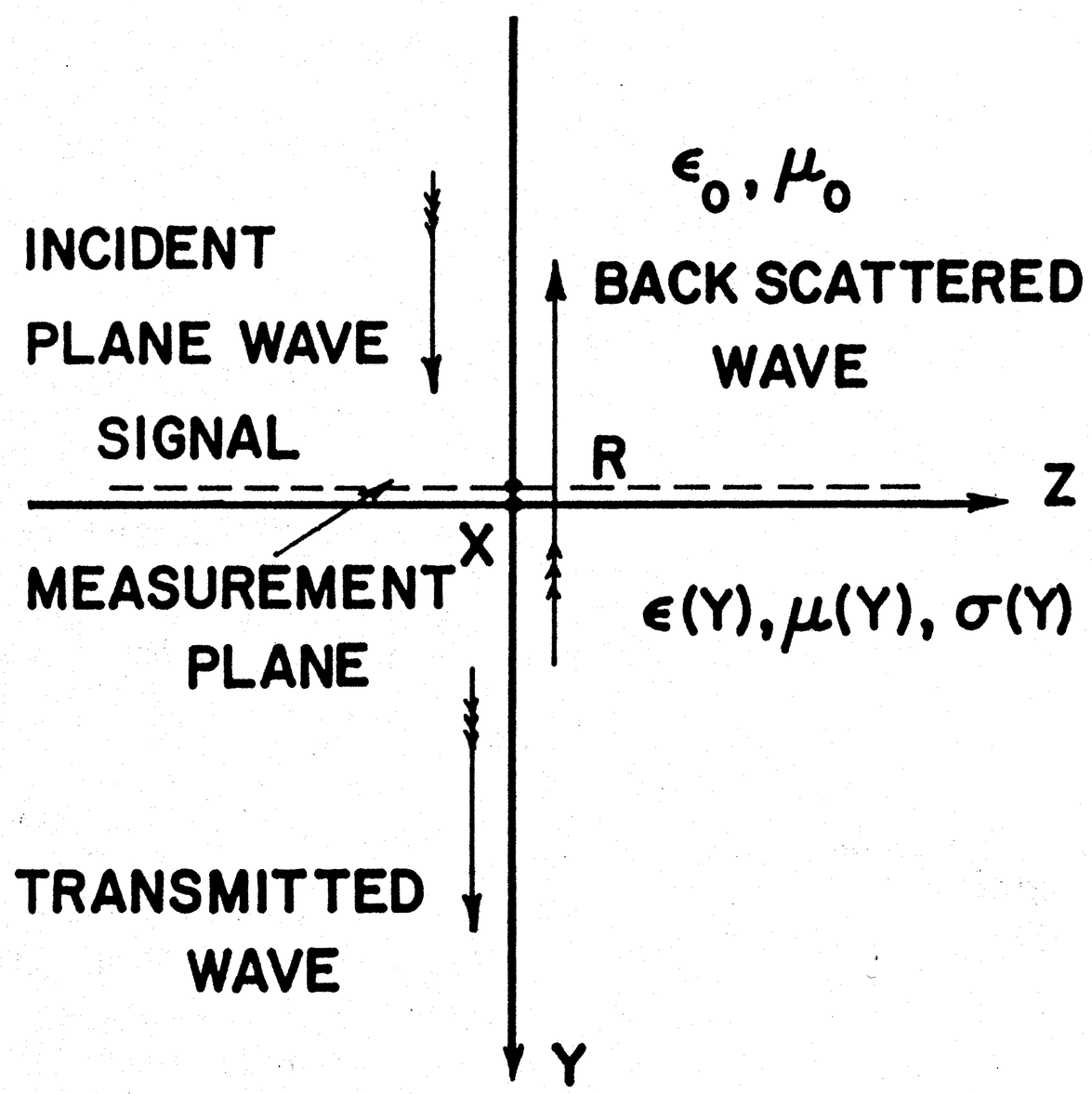


**Figure 1.** One dimensional inhomogeneous half space medium.

In the previous investigations, using a space-time discretization of an integral equation for the electric field, a solution to the layered medium profile inversion problem is studied as in [5, 6]. Here, by calculating the field at the front of the pulse in the medium, step by step, one can make an estimate of the local value of the susceptibility or conductivity. This allows the computation of the field in the next step. The disadvantage of this method is that the front of the pulse has to be traced very accurately, since the relative error in the computed field is large, especially for a lossless medium. As a result, the method is restricted to incident pulses with rather steep fronts. A modification of the above space-time discretization emphasizing space-time points where the electric field strength is relatively large is presented in [4]. The main drawback of these above methods is that they provide recovery when only one of the constitutive parameters, either conductivity or permittivity, is unknown. Also, they work best for smoothly varying profile functions.

In addition, there are different approaches in the frequency-domain adopted to solve the inverse scattering problem of interest here. In some of the frequency domain approaches [2, 3, 11], the unknown medium is described by means of a finite number of parameters in such a way that it is possible to calculate, analytically or numerically, the reflected field as a function of these parameters for a given incident field. In the case of a lossless medium, a comparison between the calculated and observed reflected field allows a direct determination of the unknown parameters. But, in general, a feedback process in conjunction with an optimization process is used for determining the set of unknown parameters that minimizes the difference between the calculated and the observed electric fields [11]. It is obvious that such an approach for a general lossy inhomogeneous medium will result in a prohibitively large number of unknown parameters for any optimization process to operate effectively with proper resolution. It should be noted here that in the frequency-domain the interaction of the entire medium with the incident field must be considered simultaneously.

In two other frequency-domain approaches [2, 3], the input data is taken as the reflection coefficient at a fixed remote location for a set of discrete frequencies. In [2] only the magnitude of the reflection coefficient is used as the input data which makes it more appealing for practical purposes. The other approach [3] uses an extension of the Born approximation to establish a Fourier integral relationship between a function of the permittivity profile and a function of the reflection coefficient at a remote location. No attempt to recover the conductivity profile, either separately or in conjunction with the permittivity profile, was made. In the method of [2], the problem of estimating the dielectric and conductivity profiles from a set of input reflected power data, was posed as a nonlinear integral equation. The equation was solved by developing a quasi-Newton iterative scheme in functional space which produces a dielectric and conductivity profile that fits the data. This iterative scheme is restricted to one dimensional cases, and from the numerical results it is clear that the performance of the scheme is not satisfactory for discontinuous profiles (for example: step jump). In fact, this seems to be the major drawback of most of the methods discussed above [1]. The alternative

method presented in this paper alleviates this drawback, in the sense any degree of resolution in the profile inversion is obtainable, and a clear systematic extension [14] to the two- and three-dimensional cases is possible including anisotropic material layers as well.

## II. NUMERICAL PROFILE INVERSION TECHNIQUE

The profile inversion technique developed in this paper is based on the differential equation formulation of the direct scattering and propagation problem referred to as the finite-difference time-domain (FD-TD) technique [7–10]. The FD-TD is a direct solution of the basic Maxwell's time-dependent curl equations for the electric and magnetic fields at a regular space lattice of points covering a volume of space containing a scatterer. A fully explicit numerical algorithm is used to simulate real time wave propagation and scattering. The electromagnetic field boundary conditions at the adjacent dissimilar layered media are automatically satisfied by the curl equations' analog. The radiation condition is not inherent, and therefore, it has been formulated separately to work appropriately in the near field and in the time-domain [13]. Using this direct scattering algorithm in conjunction with the causality of the time-domain response, an iterative optimization scheme [15] capable of estimating the electromagnetic characteristic profile in a step by step fashion, layer stripping, is developed. This optimization scheme as shown in Fig. 2, constructs the $(\sigma, \epsilon, \mu)$ profile of the one-dimensional medium such that the time history of the resulting total field at a given location, outside the medium being probed, fits a given (measured) input time-domain field response in a least-squared error sense. A brief description of the mathematical steps of the one-dimensional FD-TD formulation suitable for profile synthesis and layered inversion scheme is discussed below. Included is an efficient layer-stripping optimization scheme for the profile inversion based on causality of the exciting pulses and scattered field responses.

Various numerical case studies of the inhomogeneous one-dimensional profile inversions, namely the layered conductivity profile, the layered permittivity profile, and the simultaneous conductivity and permittivity profiles, are also presented in later sections of this paper. Further extension of the numerical case studies of the two-dimensional profile inversions [14], are reported in Part II of the accompanying paper.

### A. Summary of the One-Dimensional FD-TD Formulation

The objective of the FD-TD approach is to model the propagation of an electromagnetic wave into a volume of space containing permeable or non-permeable, dielectric and/or conducting structures which yields a flexible direct numerical volumetric scattering scheme. By time-stepping, i.e., repeatedly implementing a finite difference analog of the curl equations at each layer of the corresponding space lattice, the incident wave is tracked as it propagates through the structure and interacts with it via surface current excitation, diffusion, penetration, and diffraction. If desired for time-harmonic studies, the wave-tracking is completed

when the late-time behavior is observed at each lattice cell. The rationale for this procedure is that it achieves simplification by analyzing the interaction of the wave-front with portions of the structure surface at a given instant of time, rather than attempting a simultaneous solution of the entire problem. In fact, the numerical models for the direct electromagnetic scattering and computer algorithms implementing the FD-TD [7–10], which can treat wide classes of arbitrary shaped bodies comprised of conducting, dielectric (homogeneous, inhomogeneous, lossless, lossy) and even anisotropic media having tensor conductivity, permittivity and permeability, are presently available [10–13] with significant analytical and measurement validations.

Assuming the parameters $(\sigma, \epsilon, \mu)$ are independent of time, the following coupled scalar equations are to be solved for one-dimensional field variations with $(y, t)$ dependence:

$$\frac{\partial H_x(y,t)}{\partial t} = -\frac{1}{\mu(y)}\frac{\partial E_z(y,t)}{\partial y} \tag{1a}$$

$$\frac{\partial E_z(y,t)}{\partial t} = -\frac{1}{\epsilon(y)}\frac{\partial H_x(y,t)}{\partial y} - \frac{\sigma(y)}{\epsilon(y)}E_z(y,t) \tag{1b}$$

where $E_z(y,t)$ and $H_x(y,t)$ are the $z$ and $x$ components of the electric and magnetic fields respectively. The equations (1a) and (1b) are converted into the finite-difference form by defining [13]:

$\delta$: spatial resolution in $y$ direction

$\delta t$: time stepping increment

$$F(y,t) = F^n(j\delta, n\delta t) \tag{2a}$$

where $j$ and $n$ are integers. The centered finite-difference expressions are used for the space and time derivatives that are both second order accurate in $\delta$ and $\delta t$, respectively:

$$\frac{\partial F^n(j)}{\partial y} = [F^n(j+\frac{1}{2}) - F^n(j-\frac{1}{2})]/\delta + O(\delta^2) \tag{2b}$$

$$\frac{\partial F^n(j)}{\partial t} = [F^{n+1/2}(j) - F^{n-1/2}(j)]/\delta t + O(\delta t^2) \tag{2c}$$

To achieve the accuracy of (2b) and (2c), the components $E_z$ and $H_x$ are partitioned and interleaved about a unit cell [13] and evaluated at alternate time steps. Since in the present one-dimensional problem, Fig. 3, the fields vary along the $y$ direction only, a lattice cell is now a layer with each layer having its own homogeneous and isotropic electrical parameters. The electric field component $E_z$ is positioned at the center of each layer, while the magnetic field component $H_x$ is displaced and positioned at the interface between two adjacent layers.

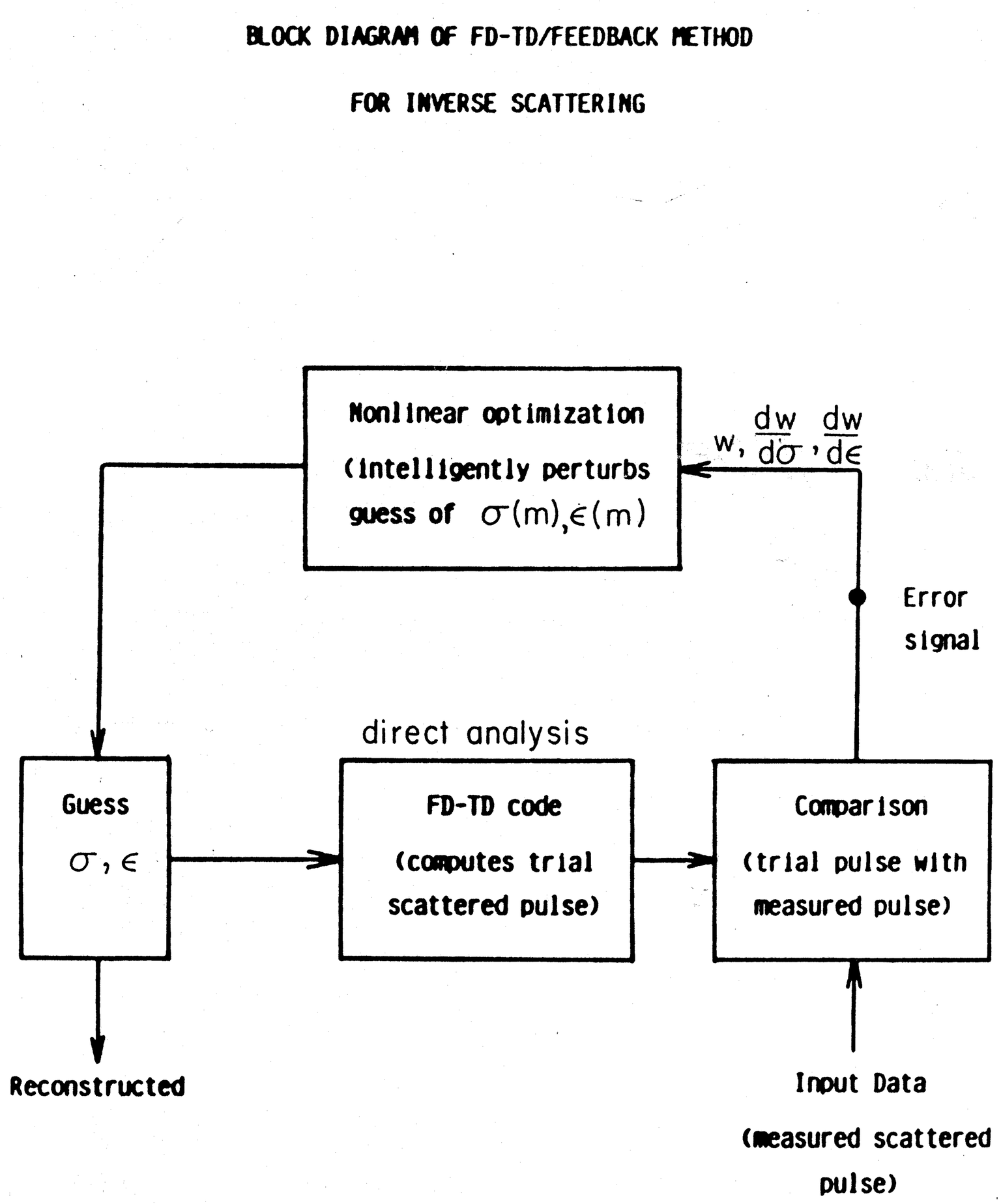


**Figure 2.** Optimization scheme for inverse scattering.

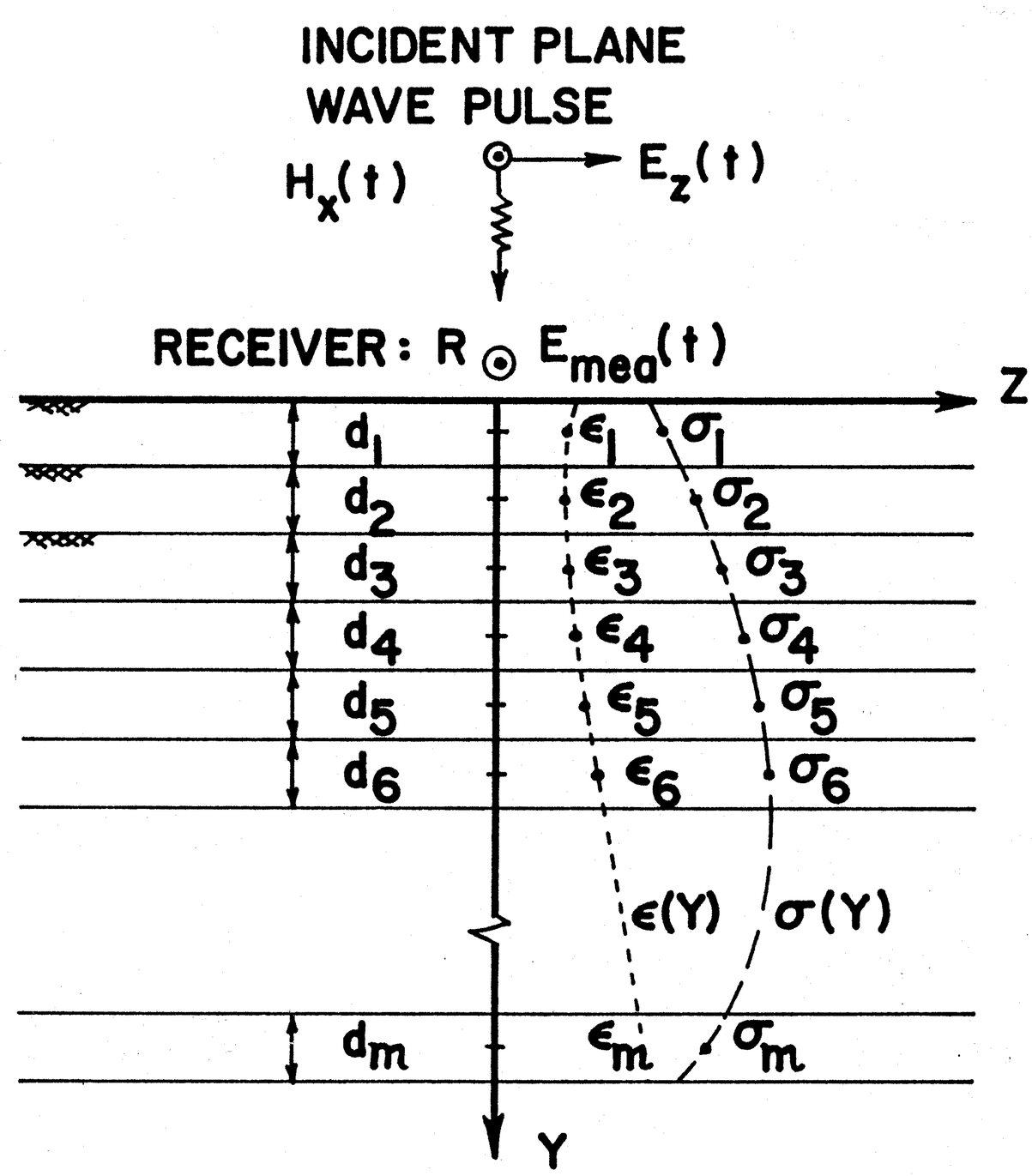


**Figure 3.** One dimensional layered medium.

Using (2b) and (2c), the coupled equations (1a) and (1b) reduce to the following finite-difference expressions using linear basis functions for the electric and magnetic field distributions:

$$H_x^{n+1/2}(j+1/2) = H_x^{n-1/2}(j+1/2) + C_1(j)[E_z^n(j) - E_z^n(j+1)] \tag{3a}$$

$$E_z^{n+1}(j) = C_2(j)E_z^n(j) + C_3(j)[H_x^{n+1/2}(j-1/2) - H_x^{n+1/2}(j+1/2)] \tag{3b}$$

where the coefficients

$$C_1(j) = \frac{\delta t}{\mu(j+1/2)\delta} \tag{3c}$$

$$C_{na}(j) = 1 - \frac{\sigma(j)\delta t}{2\epsilon(j)} \tag{3d}$$

$$C_{da}(j) = 1 + \frac{\sigma(j)\delta t}{2\epsilon(j)} \tag{3e}$$

$$C_{nb} = \frac{\delta t}{\epsilon(j)\delta} \tag{3f}$$

$$C_2(j) = \frac{C_{na}(j)}{C_{da}(j)} \tag{3g}$$

$$C_3(j) = \frac{C_{nb}(j)}{C_{da}(j)} \tag{3h}$$

With the representation given in the above equations (3a) and (3b), the field components are calculated iteratively with the new values of a field component at any layer point depending only on its previous time step and on the previous values of the components of other field at the adjacent spatial points. Hence, at any given time step, the computation of a field component will proceed one point at a time. In many electromagnetic interaction problems, including the present one, basically involve non-magnetic media. For such problems the quantity $C_1(j)$ is constant for all layers, and the coupled expressions given in (3a) and (3b) can be specialized into an efficient algorithm. Hence, defining the time stepping algorithm parameters as:

$$R = \frac{\delta t}{2\epsilon_0} \tag{4a}$$

$$R_a = \frac{\delta t^2}{\delta^2 \mu_0 \epsilon_0} \tag{4b}$$

$$R_b = \frac{\delta t}{\delta \mu_0} \tag{4c}$$

Then, the coefficients defined in (3c) to (3h) simplify to the following form:

$$C_{na}(j) = 1 - \frac{R\sigma(j)}{\epsilon_r(j)} \tag{4d}$$

$$C_{da}(j) = 1 + \frac{R\sigma(j)}{\epsilon_r(j)} \tag{4e}$$

$$C_a(j) = \frac{C_{na}(j)}{C_{da}(j)} \tag{4f}$$

$$C_b(j) = \frac{R_a}{\epsilon_r(j) + R\sigma(j)} \tag{4g}$$

and defining:

$$\tilde{E}_z^n(j) = R_b E_z^n(j) \tag{4h}$$

the one-dimensional finite-difference equations (3a) and (3b) reduces to the following time-stepping form of equations in terms of the above algorithm parameters (4a) to (4h):

$$H_x^{n+1/2}(j+1/2) = H_x^{n-1/2}(j+1/2) + [\tilde{E}_z^n(j) - \tilde{E}_z^n(j+1)] \tag{5a}$$

$$\tilde{E}_z^{n+1}(j) = C_a(j)\tilde{E}_z^n(j) + C_b(j)[H_x^{n+1/2}(j-1/2) - H_x^{n+1/2}(j+1/2)] \tag{5b}$$

The choice of space increment $\delta$ and time increment $\delta t$ is dictated by the reasons of accuracy and algorithm stability [13], respectively. To insure the accuracy of the computed spatial derivatives of the electromagnetic fields, $\delta t$ is chosen to satisfy the inequality for one-dimensional layer model:

$$\delta t \leq \frac{\delta}{c_{\max}} \tag{6}$$

$c_{\max}$: maximum wave velocity within the model.

Another basic consideration with FD-TD approach is that the present electromagnetic field problem is an "open" problem where the domain of the computed field is ideally unbounded. Clearly, for the numerical algorithms the field computation zone should be limited. Thus, the computation zone should be large enough to enclose the structure (layered medium) of interest. Further, suitable boundary conditions on the outer perimeter of the computation zone are simulated for the extension of the computation zone to infinity [12, 13].

### B. Optimization Scheme for Layer-Stripping

For the profile inversion scheme of the one-dimensional problem, the lossy inhomogeneous medium is excited by a linearly polarized pulse-transient plane wave normally incident at its interface of the outer medium, Fig. 3. The resulting time history of the total field at the receiver site $R$ is recorded and discretized into a suitable number of time steps, $M$, dependent upon the required profile resolution. Next, using the one-dimensional FD-TD formulation discussed above, the

optimization scheme [15] of Fig. 2 is utilized to construct the $(\sigma, \epsilon, \mu)$ profile of the layered medium such that at the point $R$, the resulting total field fits the recorded field (input data) in a least-square-error sense at $M$ discrete instants in time. This essentially means that the unknown inhomogeneous medium is modeled by $M$ layers of media, each of which is homogeneous within itself. It should be noted here, because the time discretization $\delta t$ of the problem is uniform, the "electrical width" of each layer $d_e$ is also uniform. However, the physical width of the layers is dependent on the corresponding relative permittivity $\epsilon_r$ and hence it is non-uniform:

$$d(j) = \frac{d_e}{[\epsilon_r(j)]^{1/2}} \tag{7}$$

Since the FD-TD formulation deals with electrical lengths as opposed to the physical lengths, the causality of marching in "uniform time steps" is assured, even with the different velocity of propagation at the different layers of the unknown medium. This is a requirement for the proposed inverse scattering formulation.

To initiate the optimization scheme for layer stripping, Fig. 2, the causality of the time marching is exploited. If the receiver is located at the media interface, as shown in Fig. 3, then at $t = 2\delta t$ only the first layer $d_1$ will contribute the total field at the point $R$, assuming the time reference $t = 0$ is considered to be the instant when the leading edge of the incident field reaches the receiver location. Thus, the only unknowns in the field calculation with FD-TD up to the time instant $t = 2\delta t$ are the unknown parameters $[\sigma(1), \epsilon(1)]$ of the first layer. For determining these unknowns, an error function $W(y,t)$ at the location $R$ is now defined as:

$$W|_{t=2n\delta t} = [E_{\text{mea}}(2n\delta t) - E_{\text{cal}}\,(2n\delta t,\ \sigma(m),\ \epsilon(m))]^2 \tag{8}$$

$E_{\text{mea}}$: total electric field measured at $R$, input data

$E_{\text{cal}}$: total electric field calculated at $R$ by FD-TD for assumed values of $\sigma(m), \epsilon(m)$

The numerical non-linear optimization algorithm [15] minimizes the error function of (8) at the location $R$ for $m = 1$, by iteratively adjusting the values of the profile characteristics $[\sigma(1), \epsilon(1)]$ of the layer $d_1$. The present non-linear optimization scheme utilized, requires the error function at the location $R$ as defined in the equation (8), and also the corresponding field gradients of the error function at the location $R$ calculated with respect to the unknown characteristic parameters $\sigma(m)$ and $\epsilon(m)$ of the $m^{\text{th}}$ layer being probed, as defined below. Hence, at the location $R$, the gradient of the error function with respect to the unknown conductivity parameter is given by:

$$\frac{\partial W(j=R,m)}{\partial \sigma(m)}\Big|_{t=2n\delta t} = -2[E_{\text{mea}} - E_{\text{cal}}]G_z(j=R,m) \tag{9a}$$

$$P_x^n(j,m) = \frac{\partial H_x^n(j)}{\partial \sigma(m)} \tag{9b}$$

$$G_z^n(j,m) = \frac{\partial E_z^n(j)}{\partial \sigma(m)} \tag{9c}$$

$$\tilde{G}_z^n(j,m) = R_b G_z^n(j,m) \tag{9d}$$

In terms of the above algorithm parameters (9a) to (9d), the following one-dimensional finite-difference expressions are obtained for the gradient function in time-stepping form:

$$P_x^{n+1/2}(j+1/2,m) = P_x^{n-1/2}(j+1/2,m) + [\tilde{G}_z^n(j,m) - \tilde{G}_z^n(j+1,m)] \tag{9e}$$

$$\begin{aligned}\tilde{G}_z^{n+1}(j,m) =& C_a(j)\tilde{G}_z^n(j,m) + C_c(j,m)\tilde{E}_z^n(j) \\ &+ C_b(j)[P_x^{n+1/2}(j-1/2,m) - P_x^{n+1/2}(j+1/2,m)] \\ &+ C_d(j,m)[H_x^{n+1/2}(j-1/2) - H_x^{n+1/2}(j+1/2)]\end{aligned} \tag{9f}$$

where

$$\begin{aligned}C_c(j,m) &= \frac{\partial C_a(j)}{\partial \sigma(m)} && \text{for } j = m \\ &= 0 && \text{for } j \neq m\end{aligned} \tag{9g}$$

$$\begin{aligned}C_d(j,m) &= \frac{\partial C_b(j)}{\partial \sigma(m)} && \text{for } j = m \\ &= 0 && \text{for } j \neq m\end{aligned} \tag{9h}$$

Similarly, at the location $R$, the gradient of the error function with respect to the unknown permittivity parameter is given by:

$$\frac{\partial W(j=R,m)}{\partial \epsilon(m)}\Big|_{t=2n\delta t} = -2[E_{\text{mea}} - E_{\text{cal}}]T_z(j=R,m) \tag{10a}$$

$$S_x^n(j,m) = \frac{\partial H_x^n(j)}{\partial \epsilon(m)} \tag{10b}$$

$$T_z^n(j,m) = \frac{\partial E_z^n(j)}{\partial \epsilon(m)} \tag{10c}$$

$$\tilde{T}_z^n(j,m) = R_b T_z^n(j,m) \tag{10d}$$

Again, in terms of the above algorithm parameters (10a) to (10d), the following second set of one-dimensional finite-difference expressions are obtained for the gradient function in time-stepping form:

$$S_x^{n+1/2}(j+1/2,m) = S_x^{n-1/2}(j+1/2,m) + [\tilde{T}_z^n(j,m) - \tilde{T}_z^n(j+1,m)] \tag{10e}$$

$$\begin{aligned}\tilde{T}_z^{n+1}(j,m) =& C_a(j)\tilde{T}_z^n(j,m) + C_e(j,m)\tilde{E}_z^n(j) \\ &+ C_b(j)[S_x^{n+1/2}(j-1/2,m) - S_x^{n+1/2}(j+1/2,m)] \\ &+ C_f(j,m)[H_x^{n+1/2}(j-1/2) - H_x^{n+1/2}(j+1/2)]\end{aligned} \tag{10f}$$

$$C_e(j,m) = \frac{\partial C_a(j)}{\partial \epsilon(m)} \quad \text{for } j = m$$
$$= 0 \quad \text{for } j \neq m \tag{10g}$$
$$C_f(j,m) = \frac{\partial C_b(j)}{\partial \epsilon(m)} \quad \text{for } j = m$$
$$= 0 \quad \text{for } j \neq m \tag{10h}$$

Similarly, at the time instant $t = 4\delta t$, the first two layers $m = 1, 2$ with resolution depths $d_1$ and $d_2$ take part in the electromagnetic interaction. However, now the characteristics of the first layer $d_1$ is known, and thus by iterative optimization the characteristic parameters of the second layer $d_2$ are recovered. The process is continued for the remaining layers. Some observations regarding the numerical implementation of the above layer stripping scheme are as follows:

(a) As a first step, the time interval $\delta t$ can be made large and a coarse profile estimate of the electromagnetic characteristics of the medium is obtained. In this estimate, the region where the profile appears to be changing rapidly, can be recalculated by using a finer sub-intervals of the time step in the corresponding region of the measured time-history of the total electric field at the point $R$. This variable resolution is effective and accurate at the same time.
(b) When the $m^{\text{th}}$ layer's profile is being recovered, all the non-zero field information up to the time instant $2(m-1)\delta t$ is known from the previous optimization step, stripping of the $(m-1)^{\text{th}}$ layer, and these values are not affected by the changes in $\sigma(m)$ and $\epsilon(m)$ due to causality. Thus, in the $m^{\text{th}}$ optimization step, the field values obtained in the earlier optimization steps are of direct use.
(c) Since the FD-TD formulation gives field values at all the grid points of the layered geometry, the field values inside the layer medium can be successively monitored to determine the depth at which the profile recovery scheme should be terminated, i.e., the depth into the medium at which the field due to the transmitted pulse has decayed sufficiently to produce no significant scattering contributions.

## III. PROFILE INVERSION RESULTS

Based on the detailed profile inversion technique developed above involving the FD-TD [13] and the optimization scheme [15], selected numerical results are presented to demonstrate applicability of the layer-stripping procedure for one-dimensional inverse scattering. Several case studies involving pure conductivity profiles, pure permittivity profiles, and also combinations of both the conductivity and permittivity profiles have been investigated. Some of the generic profile distributions, namely, rectangular, triangular, saw-tooth, and sinusoidal profile distributions have been recovered.

For the profile inversion scheme, the input data consists of the recorded time history of the total electric field at the receiver site $R$ located in front of the medium being probed. The recorded data at the receiver site $R$ for different

profile distributions are shown in Figs. 4a, 5a and 6. In fact, the recorded data utilized is completely noise free and was obtained by direct time-domain scattering problem with very high resolution of a sinusoidal half-pulse excitation. Generally, practical input data when measured will include random noise distributions depending on the transient measurements. No attempt has been made in this paper to include any noise study. All questions concerning input data with random noise distributions, effect of different pulse excitations, limits and accuracy of the data recovered, in fact, are addressed and reported in a separate study [14] involving accurate reconstruction of two-dimensional target shapes from a single point TM-scattered field pulse response.

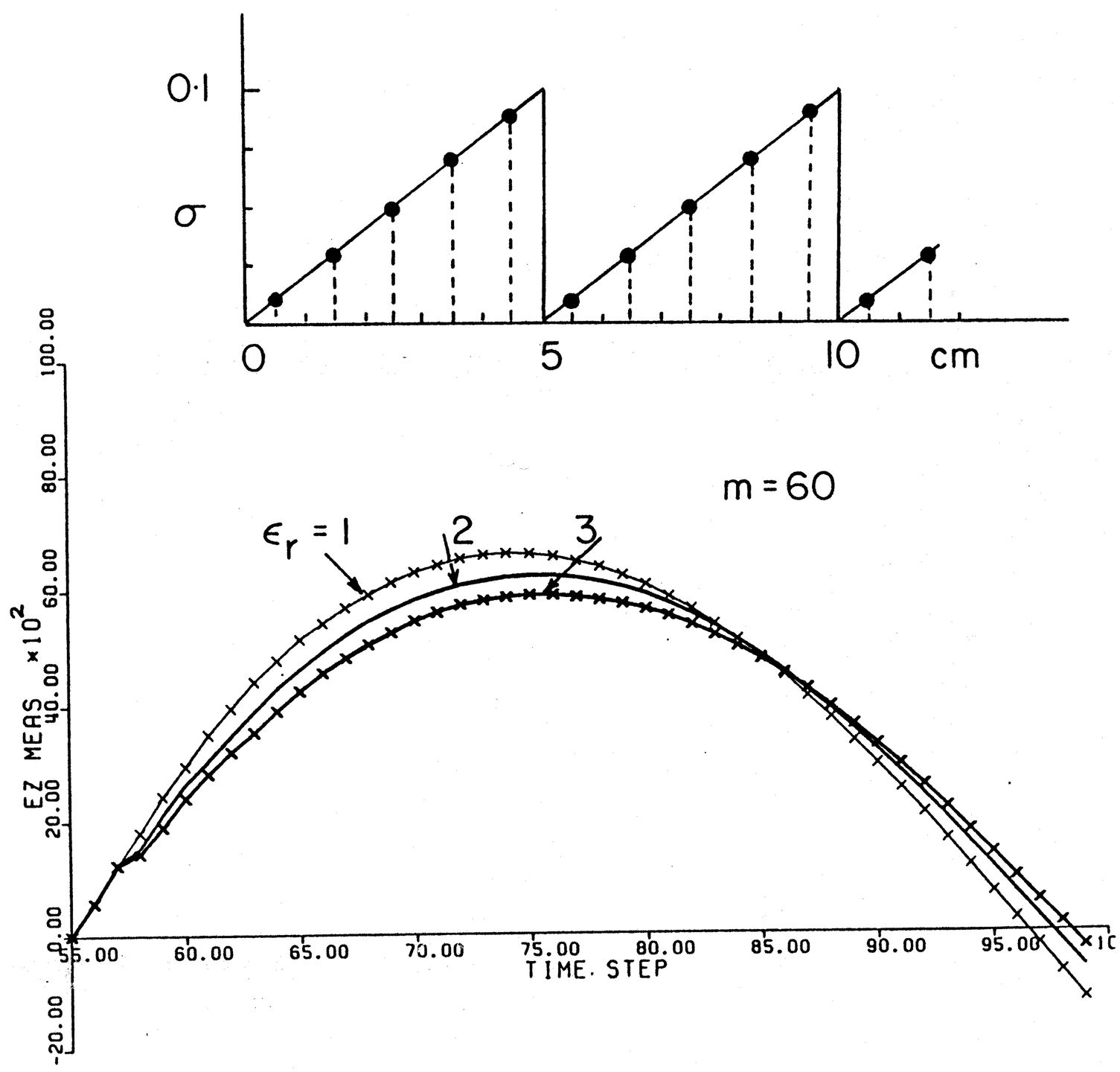


**Figure 4a.** Recovery on saw-tooth conductivity profile and the electric field input data.

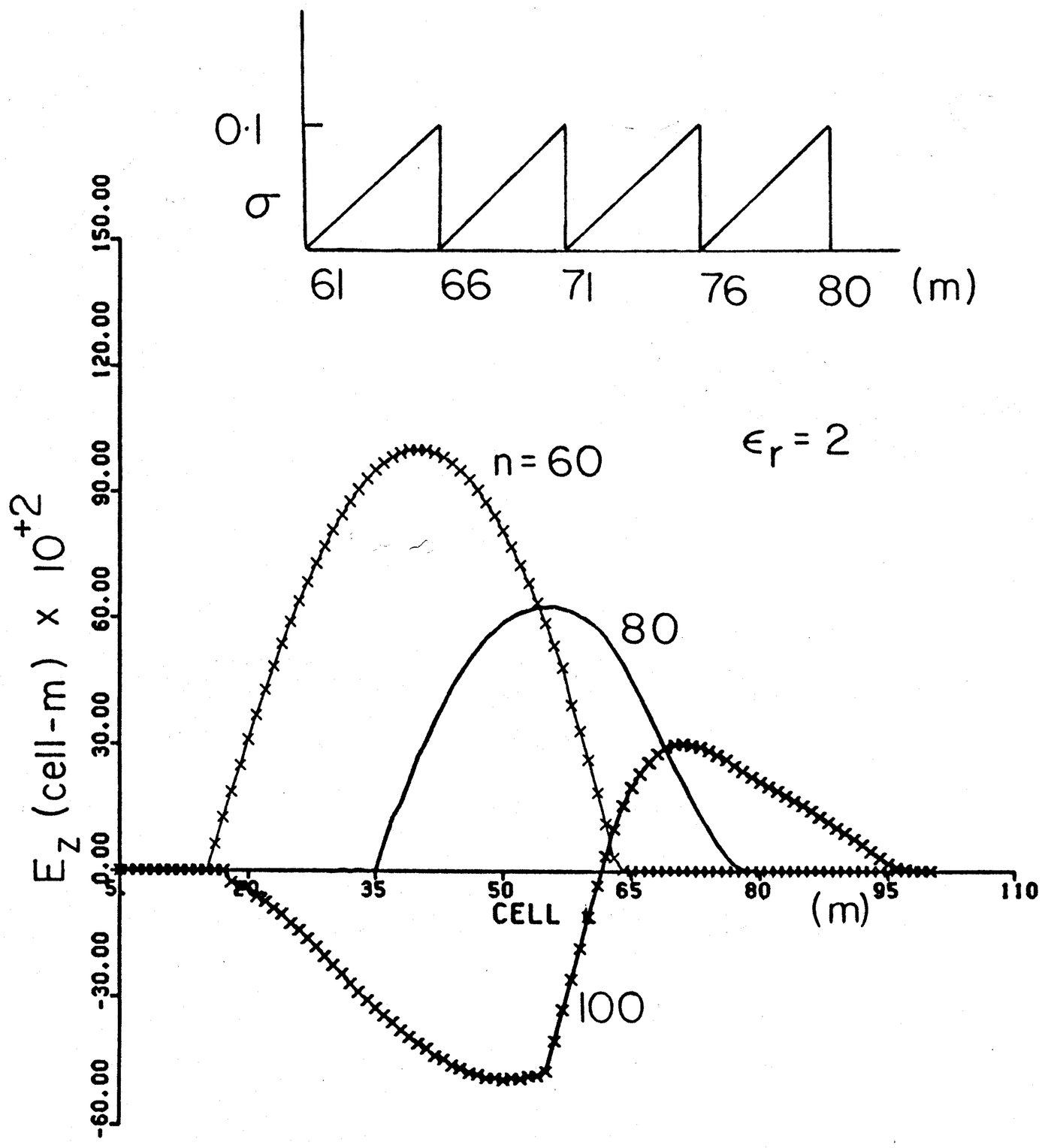


**Figure 4b.** Spatial distribution of the electric field associated with conductivity profile.

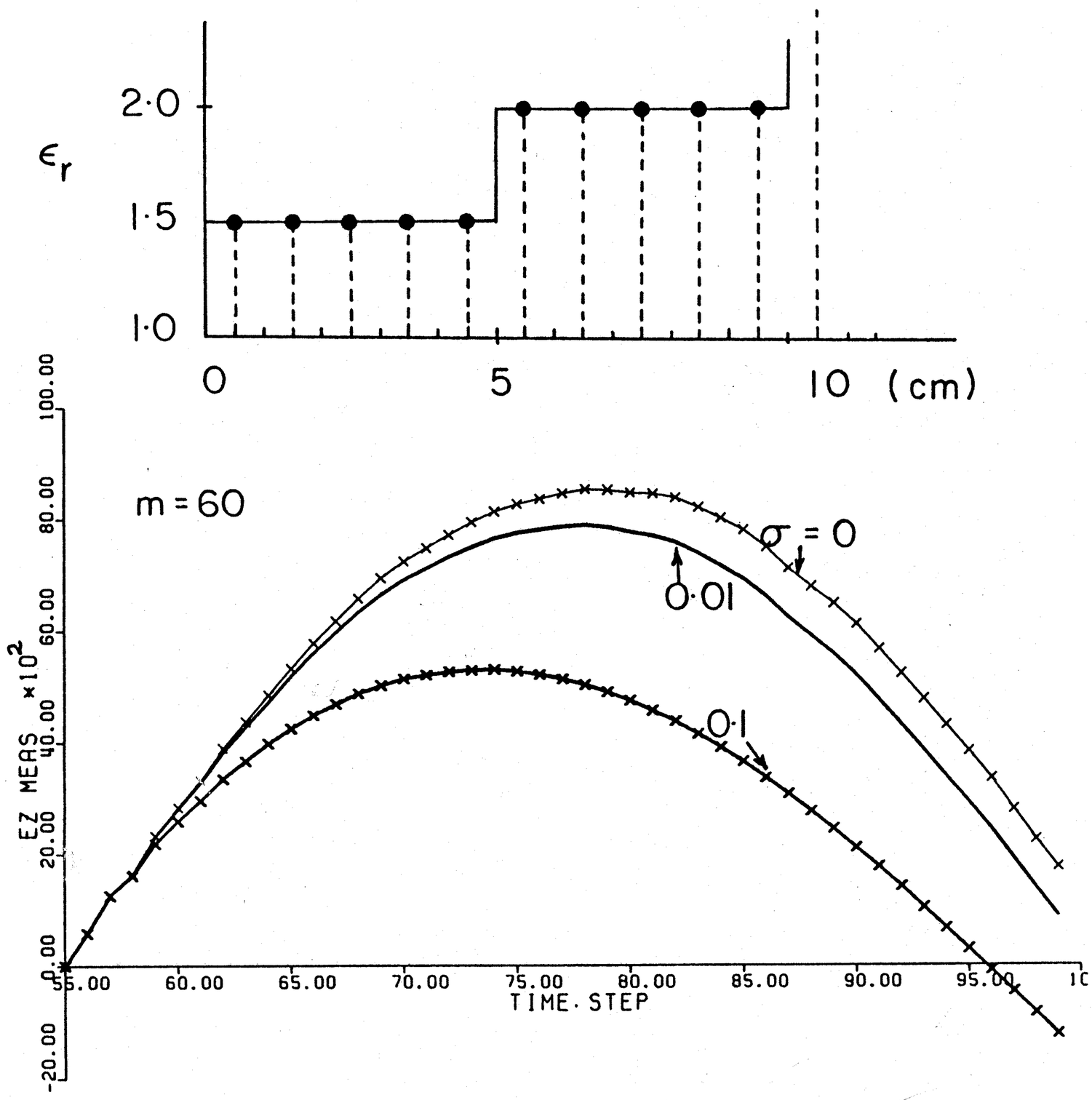


**Figure 5a.** Recovery stair-case permittivity profile and the electric field input data.

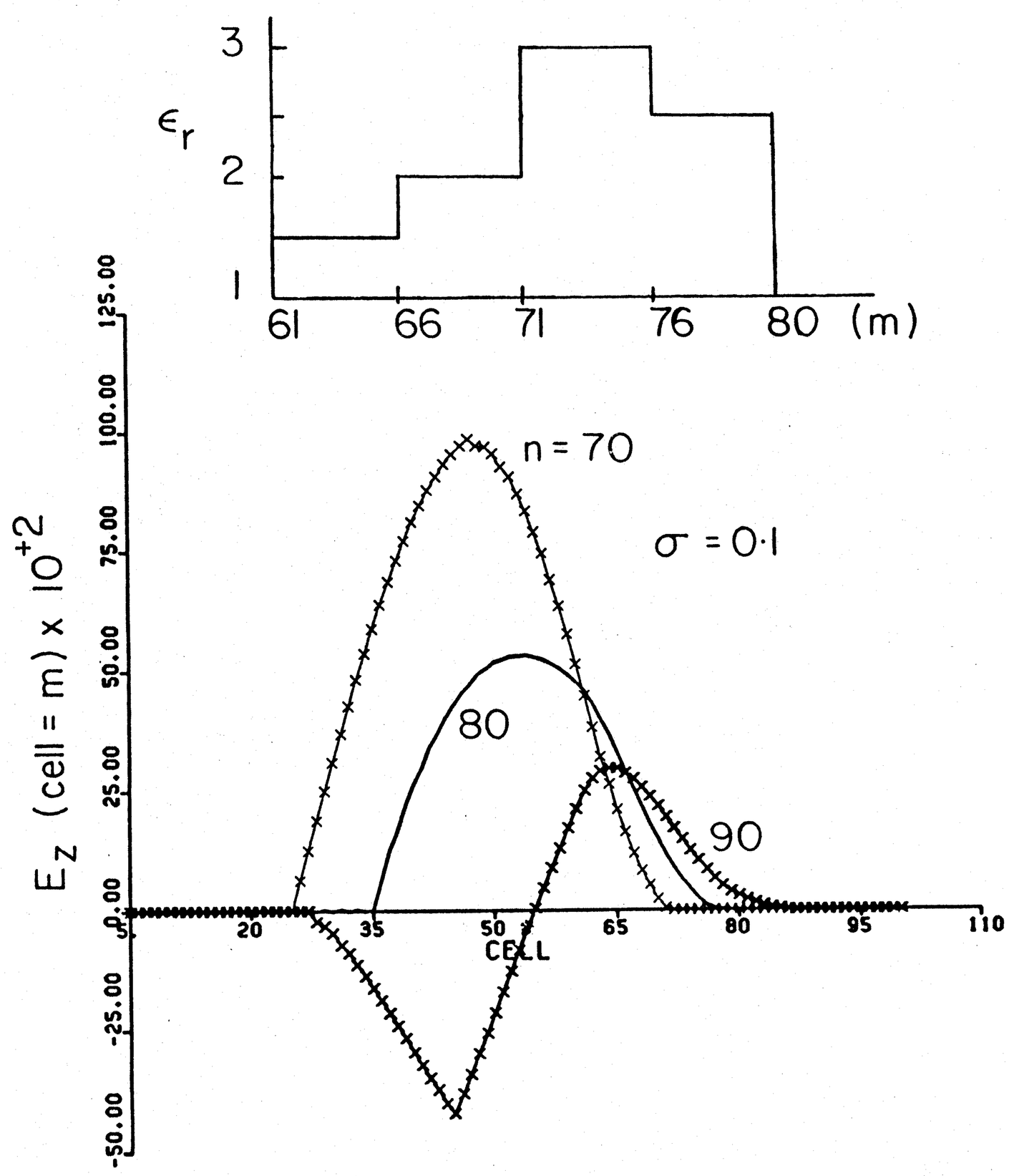


**Figure 5b.** Spatial distribution of the electric field associated with permittivity profile.

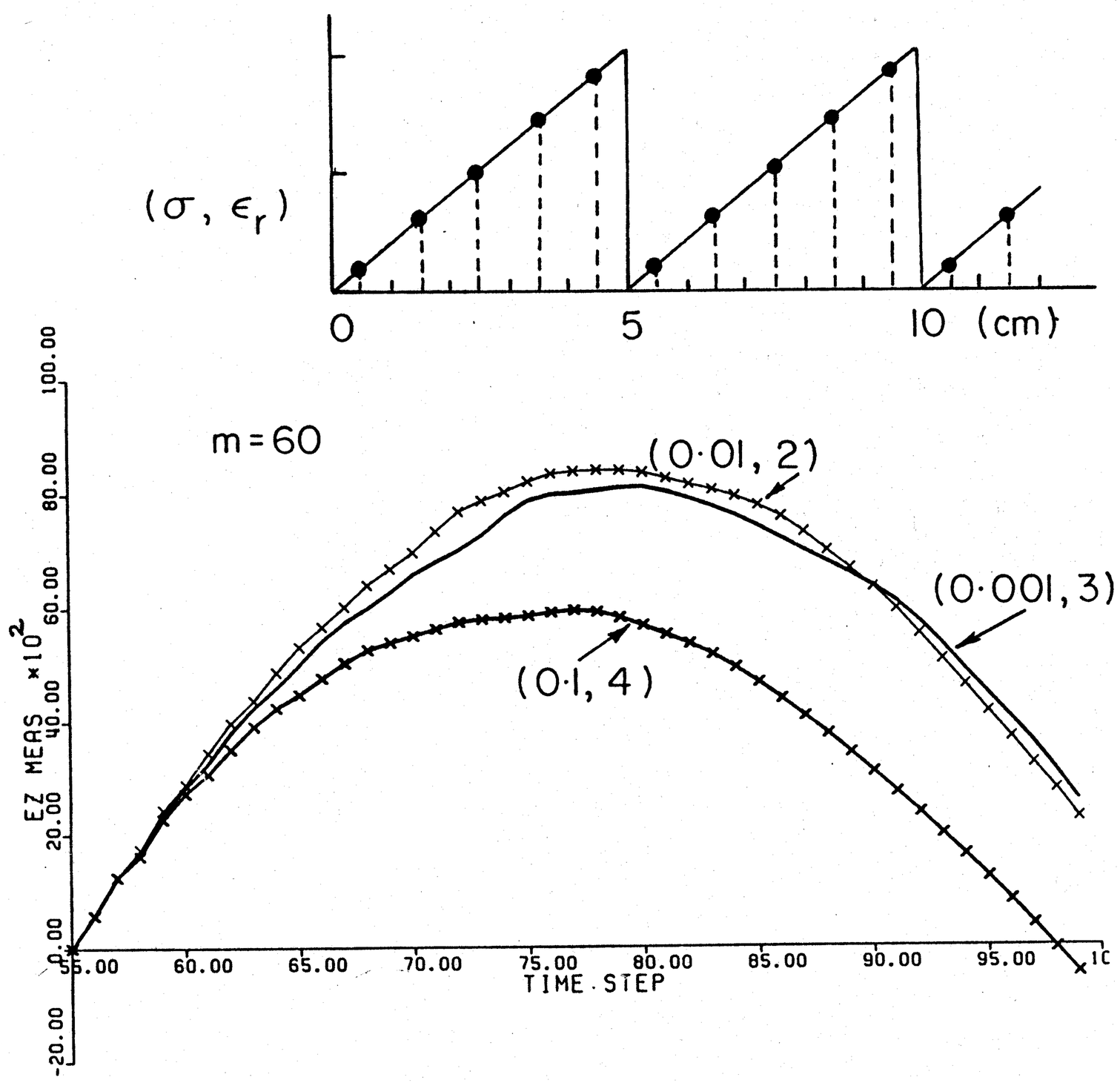


**Figure 6.** Recovery on saw-tooth conductivity and permittivity profile and the electric field input data.

The Fig. 4a shows results of the conductivity profile recoveries. The exciting incident pulse used is a half-cycle sinusoid at 300 MHz. The results are recovered with a spatial resolution of 0.01 meter in the region outside the medium being probed, and also the same physical resolution is utilized within the medium being probed. The source is located at the $5^{th}$ spatial layer and is turned on at the time instant $t = 0$. With the spatial resolution of 0.01 meter, the field observation or measurement point $R$ is situated at the $60^{th}$ spatial layer or same as just one layer in front of the medium being probed. The Fig. 4a shows results of the first ten layers stripping corresponding to the two cycles of the saw-tooth profile, 0.1 meter thick, recovered based on the numerical algorithm described earlier. Numerical difficulties are encountered for probing deeper layers due to low scattering returns from the deep layers. In order to overcome this limitation, it is necessary to use low frequency half sinusoid exciting pulses, or the alternative pulse shapes such as the gaussian and its derivatives. The Fig. 4b shows spatial distribution of the total $z$ component of the electric field at selected time instants.

Similarly, the Fig. 5a shows corresponding results of the permittivity profile recoveries and the Fig. 5b shows the spatial distribution of the total $z$ component of the electric field at few selected time instants. The permittivity profile investigated is that of the stair-case distribution. From numerical point of view, it is observed the layer stripping algorithm converges slower for the permittivity profiles than for the case of conductivity profiles, and rate of convergence is also affected with respect to the deep layers being probed. The results of Fig. 6 correspond to an interesting case of simultaneous recovery of both conductivity and permittivity profiles. The conductivity and the permittivity profiles considered are having saw-tooth distributions as a function of depth. Three different cases of the input data are investigated with peak values of the parameters as shown in the Fig. 6. The convergence rate of the optimization scheme is slow compared to the single parameter layer stripping examples presented in this paper. Even though the results presented are for the case of half-sinusoid input pulse, the procedure discussed is applicable for any other pulse input waveforms. Detailed studies are still underway concerning the application of different excitation pulse shapes. In fact, the present numerical algorithm is also suited for other characteristic parameters such as the permeability distributions. These will be reported separately along with noise study in the input data [14]. These examples thus demonstrate the flexibility of the present inversion scheme, which not only works for smooth profiles but also can recover discontinuous profiles as well.

## IV. CONCLUSIONS

This paper illustrated an efficient and simple numerical scheme for the inverse scattering problem of determining the electromagnetic characteristics, namely, the conductivity and permittivity of the layered one-dimensional profiles. The numerical algorithms developed here are quite useful for layered material synthesis.

This approach is quite general and can be easily extended to two- and three-dimensional problems by appropriately replacing the forward scattering algorithm with the two- and three-dimensional FD-TD scheme.

## ACKNOWLEDGMENTS

This research work was supported partially by the Office of Naval Research (ONR) under grant No. N00014-88-K-0475 and by the National Science Foundation (NSF) under grant No. ASC-8811273.

The Editor thanks C. Lee, D. Lesselier, W. Tabbara, and A. G. Tijhuis for reviewing the paper.

## REFERENCES

1. Bolomey, J. Ch., D. Lesselier, C. Pichot , and W. Tabbara, "Spectral and time domain approaches to some inverse scattering problems," *IEEE Trans. Antennas and Propagat.,* Vol. AP-29, No. 2, 206–212, March 1981.
2. Coen, S., K. K. Mei, and D. J. Angelakos, "Inverse scattering technique applied to remote Sensing of Layered Media," *IEEE Trans. Antennas and Propagat.,* Vol. AP-29, No. 2, 298–306, March 1981.
3. Tabbara, W., "Reconstruction of permittivity profiles from a spectral analysis of the reflection coefficient," *IEEE Trans. Antennas and Propagat.,* Vol. AP-27, No. 2, 241–244, March 1979.
4. Tijhuis, A. G., "Iterative determination of permittivity and conductivity profiles of a dielectric slab in the time domain," *IEEE Trans. Antennas and Propagat.,* Vol. AP-29, No. 2, 239–245, March 1981.
5. Bolomey, J. Ch., C. Durix, and D. Lesselier, "Determination of conductivity profiles by time domain reflectometry," *IEEE Trans. Antennas and Propagat.,* Vol. AP-27, No. 2, 244–248, March 1979.
6. Lesselier, D., "Determination of index profiles of time-domain reflectometry," *Journal of Optics,* Vol. 9, 349–358, December 1978.
7. Taflove, A., and K. Umashankar, "A hybrid moment method/ finite-difference time-domain approach to electromagnetic coupling and aperture penetration into complex geometries," *IEEE Trans. Antennas and Propagat.,* Vol. AP-30, No. 4, 617–627, July 1982.
8. Umashankar, K., and A. Taflove, "A novel method to analyze electromagnetic scattering of complex objects," *IEEE Trans. Electromagnetic Compatibility,* Vol. EMC-24, 397–405, November 1982.
9. Taflove, A., and K. Umashankar, "Radar cross section of general three-dimensional scatterers," *IEEE Trans. Electromagnetic Compatibility,* Vol. EMC-25, 433–440, November 1983.
10. Umashankar, K., and A. Taflove, "Analytical models for electromagnetic scattering," Final Report, Contract No. F19628-82-C-0140, Rome Air Development Center, Hanscom Airforce Base, Ma. June 1984.
11. Mostafavi, M., and R. Mittra, "Remote probing of inhomogeneous media using parameter optimization techniques," *Radio Science,* Vol. 7, No. 12, 1105–1111, December 1972.
12. Mur, G., "Absorbing boundary conditions for the finite-difference approximation of the time-domain electromagnetic field equations," *IEEE Trans. Electromagnetic Compatibility,* Vol. EMC-23, 377–382, November 1981.

13. Taflove, A., and K. Umashankar, "User codes for the finite-difference time-domain method," Final Report, RADC-TR-82-16, Rome Air Development Center/ GAFB, February 1982.
14. Strickel, M., A. Taflove and K. Umashankar, "Finite-difference time-domain formulation of an inverse scattering scheme for remote sensing of conducting and dielectric targets: Part - II two dimensional case," *J. of Electromagnetic Waves and Applica.*, to appear, 1994.
15. Fletcher, R., "A new approach to variable metric algorithms," *Computer Journal*, Vol. 13, 317–322, 1970.

**Korada Umashankar** received the B.E. degree from Mysore University and M.E. degree from Indian Institute of Science, Bangalore, India and Ph.D. degree from University of Mississippi, all in Electrical Engineering. From 1975 to 1977 he was with faculty of University of Mississippi, from 1977 to 1979 with Airforce Weapons Lab., KAFB, Albuquerque and from 1979 to 1984 a staff member in the Electronics Division, IIT Research Institute, Chicago, Illinois. During 1984, he joined University of Illinois at Chicago where he is a Professor of Electrical Engineering and Computer Science. He has authored three text books. Dr. Umashankar is a member of Eta Kappa Nu, Sigma Xi, URSI Commission B, and a Senior member of IEEE.

**Sujeet Chaudhuri** was born in Calcutta, India, on August 25, 1949. He received the B.E. degree from Birla Institute of Technology and M.Tech. degree from Indian Institute of Technology, Delhi, India, in 1970 and 1972. Further, he received the M.Sc., and Ph.D. degrees from University of Manitoba, Canada, in 1973 and 1977 respectively. In 1977, he joined University of Waterloo, Waterloo, Canada where he is a Professor of Electrical Engineering and Computer Science. Dr. Chaudhuri is a member of URSI Commission B and a Senior member of IEEE.

**Allen Taflove** was born in Chicago, Illinois, on June 14, 1949. He received the B.S., M.S., and Ph.D., degrees in Electrical Engineering from Northwestern University, Evanston, Illinois in 1971, 1972, and 1975, respectively. From 1975 to 1984, he was a staff member in the Electronics Division, IIT Research Institute, Chicago, Illinois. During 1984, he returned to Northwestern University where he is a Professor of Electrical Engineering and Computer Science. He has authored two text books. Dr. Taflove is a member of Tau Beta Pi, Eta Kappa Nu, Sigma Xi, URSI Commission B, The Electromagnetics Academy, and a Fellow of IEEE.